Invited Paper

Volume Bragg Gratings as Ultra-Narrow and Multiband Optical Filters

Alexei L. Glebov*[a], Oleksiy Mokhun[a], Alexandra Rapaport[b#], Sébastien Vergnole[b], Vadim Smirnov[a], Leonid B. Glebov[a]
[a]OptiGrate Corp, 3267 Progress Dr., Orlando, FL 32826, USA;
[b]Horiba Scientific, 231 rue de Lille, 59650 Villeneuve d'Ascq, France

ABSTRACT

High efficiency volume Bragg gratings (VBGs) in photo-thermo-refractive (PTR) glass provide unmatched optical filtering capabilities with optical densities as high as 50 dB and linewidths as narrow as 1 cm^{-1}. In this work we review recent advances in VBG technologies that enabled key improvements of high efficiency grating properties and led to development of unique VBG based optical filters for Raman spectroscopy and other applications. Such narrow band notch and bandpass filters make ultra-low frequency Raman measurements possible with single stage spectrometers, therefore, largely improving optical throughput of high end Raman instruments while reducing complexity of the measurements. In this work we also present novel volume multiplexed ultra-narrow band VBG filters with high reflection at multiple wavelengths. Such multiband holographic optical elements are formed by overlapping of several high efficiency VBGs in a single glass plate. Raman spectra obtained with multiband VBG filters and single stage spectrometers, show unmatched capability of the filters to provide simultaneous access to Stokes and anti-Stokes Raman modes with frequencies as low as 5 cm^{-1} at different wavelengths.

Keywords: volume Bragg gratings, narrow band optical filters, multiband notch filters, holographic optical elements, Raman spectroscopy, THz frequency vibration measurements, low wavenumber spectroscopy

1. INTRODUCTION

Volume Bragg gratings (VBGs) in photo-thermo-reflective (PTR) glass has been used for various applications, such as longitudinal and transverse mode selection in diode [1,2], fiber [3,4], solid-state laser resonators [5,6], stretchers and compressors for picosecond and femtosecond lasers [7,8], mirrors for high brightness dense spectral beam combining [9,10], angular beam deflectors/magnifiers [11] and so on. Theoretical and experimental studies of VBGs, their properties and applications can be found in multiple references (e.g., [12, 13]). A possibility to make much thicker VBGs in PTR glass compared to polymer based materials or thin oxide and semiconductor films allows fabrication of optical filters with linewidths orders of magnitude narrower than those by other techniques.

In recent years, VBG optical filters found their use in Raman spectroscopy [14-17]. The ultra-narrow linewidth of VBG-based bandpass and notch filters enabled dramatic modification of Raman spectrometers for low-frequency measurements. Prior to introduction of VBG bandpass and notch filters [14, 15], low frequency Raman measurements (< 50 cm^{-1}) were performed primarily with two techniques: 1) triple-stage monochromators, in which the double-subtractive spectrometer is used to reject the laser line as close as 2-3 cm^{-1} from the laser source center wavelength; 2) Iodine gas filters, in which I_2 gas stabilized at a certain temperature absorbs very narrow laser line. VBG based filters, or Bragg filters can provide access to such ultra-low frequency (ULF) vibrations in a much simpler and more stable way [15]. Studies of vibrations in the terahertz range (5-100 cm^{-1}) are critical for analysis of many materials such as graphene [16], semiconductor superlattices [17], carbon nanotubes, proteins, amorphous glasses, and many others.

In this paper we review volume Bragg gratings in PTR glass and their unique properties and applications for narrow band optical filtering. Also, for the first time we demonstrate multiplexing of two high reflecting VBGs with diffraction efficiencies exceeding 99.9% and bandwidth at FWHM (full width at half maximum) less than 3 cm^{-1} in one piece of PTR glass. Such Bragg filters provide sufficient Rayleigh light rejection at two wavelengths so that ultra-low frequency measurements become possible with a single stage Raman spectrometer with multiple laser sources.

*aglebov@optigrate.com; www.optigrate.com; [#]AR's current address: Eolite Systems, 11 avenue Canteranne, 33600 Pessac, France

Micro-Optics 2012, edited by Hugo Thienpont, Jürgen Mohr, Hans Zappe, Hirochika Nakajima,
Proc. of SPIE Vol. 8428, 84280C · © 2012 SPIE · CCC code: 0277-786X/12/$18 · doi: 10.1117/12.923575

2. PHOTO-THERMO-REFRACTIVE GLASS

VBG is a volume hologram recorded in a bulk of PTR glass by exposure to the interference pattern formed by the UV laser radiation at 325 nm [12]. PTR glass is a Na_2O-ZnO-Al_2O_3-SiO_2 glass doped with silver (Ag), cerium (Ce), and fluorine (F). The photo-thermal-refractive process is based on precipitation of dielectric microcrystals of NaF in the glass bulk. The process proceeds in several steps. The first step is exposure of the glass to near UV radiation to photo-excite cerium ions. The Ce^{3+} ions convert to Ce^{4+} and the released electrons are trapped by silver ions converting them to neutral silver atoms. This second stage corresponds to latent image formation in conventional photo-materials and no significant coloration or refractive index variations occur at this stage. The latent image corresponds to a distribution of silver atoms in the glass bulk that matches the absorbed dosage spatial distribution of photo-exciting radiation. The third stage is diffusion of silver atoms, which leads to creation of tiny particles containing silver at temperatures exceeding 450ºC. These particles containing silver serve as nucleation centers for sodium fluoride crystal growth at temperatures exceeding 500˚C.

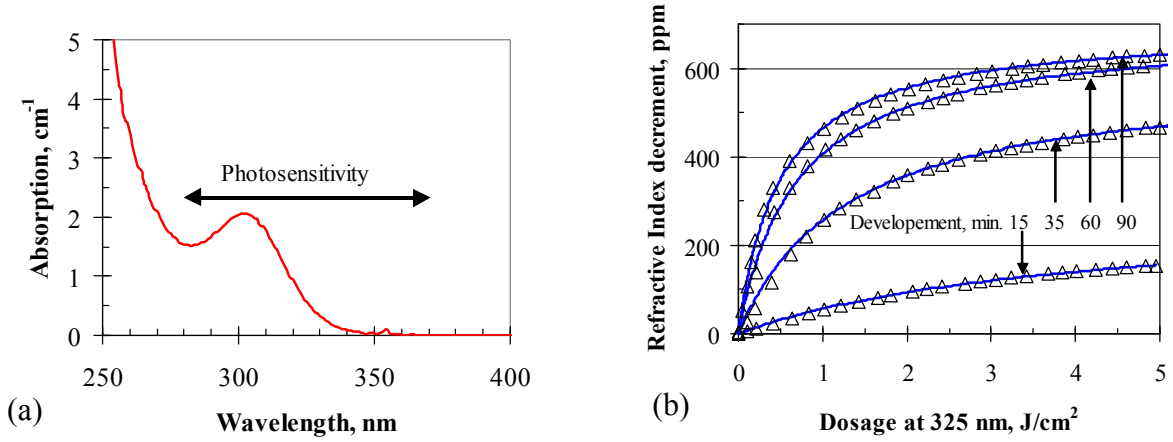

Figure 1. (a) Absorption spectrum of PTR glass showing the region of glass photosensitivity. On the long wavelength side PTR glass is transparent up to 2.5 µm. (b) Dependence of the photoinduced refractive index increment in PTR glass as a function of PTR sample irradiation at 325 nm for different thermal development times.

Fig. 1(a) depicts an absorption spectrum of PTR glass in UV region. Photosensitivity of PTR glass is determined by the absorption band of Ce^{3+}. The band maximum is centered at 305 nm and extends approximately from 280 to 350 nm. The window of complete transparency of PTR glass is from 350 to 2700 nm. Absorption at wavelengths > 2700 nm is produced by hydroxyl groups contained in silicate glass as technological contaminations. Induced refractive index change, depicted in Fig. 1(b), as a function of energy dosage of exposure exhibits a continuously decreasing slope which is modeled by hyperbolic functions. One can see that increasing the time of thermal development increases the initial slope of the dependencies which leads to increasing the actual photosensitivity. However, further development leads to saturation of the induced index of refraction. The figure shows that a given value of the refractive index modulation or increment can be achieved by various combinations of exposure dosages and development times. It should also be noted that the presented curves are for a fixed photosensitivity value of PTR glass. The PTR glass photosensitivity can also be modified in the glass fabrication process, thus, providing an additional control mechanism that can affect the final properties of VBGs. Hence, a proper choice of glass's intrinsic photosensitivity, holographic exposure and thermal development parameters allows for achieving optical characteristics of VBGs.

PTR glass is a crown-type optical glass having a refractive index at 587.5 nm of n_d=1.4959 and Abbe number ν_δ=59.2. Thermal variations of refractive index in PTR glass are very low (dn/dT=5×10^{-8} 1/K). This feature leads to a thermal shift of Bragg wavelength in PTR diffractive gratings of 7 pm/K. The fact that refractive index modulation in PTR glass is not produced by a photo-induced process but caused by thermal precipitation of a crystalline phase, leads to an important consequence. There is no way to destroy crystalline particles of NaF in glass matrix by any type of radiation. This is why PTR holograms are stable under exposure to IR, visible, UV, X-ray, and gamma-ray irradiation. VBGs in PTR glass also demonstrate superior environmental stability as the silicate glass matrix is not susceptible to humidity degradation and the holographic image formed in PTR glass cannot be thermally damaged up to 400°C.

3. REFLECTING VOLUME BRAGG GRATINGS

A diffractive grating produced by refractive index modulation in the volume of a photosensitive material is called a volume Bragg grating. Depending on the diffraction angle, orientation of a grating in the plate, and the period modulation of the grating one can distinguish several types of Bragg gratings. A grating is called a transmitting Bragg grating (TBG) if the diffracted beam crosses the back surface, reflecting Bragg grating (RBG) - if the diffracted beam crosses the front surface. In case of a chirped Bragg grating (CBG), the period of the grating varies either along or across the beam propagation direction. A reflecting VBG consists of parallel plane grating surfaces of modulated refractive index in PTR glass as it is schematically shown in Figure 2.

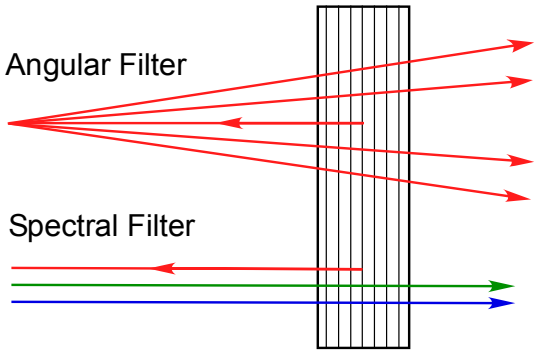

Figure 2. Schematics of a reflecting volume Bragg grating (RBG). RBG is a narrow band spectral and angular filter that allows selection of a narrow spectral region of light within an acceptance angle determined by the Bragg conditions.

RBGs have a dual function of a narrow band spectral filter as well as angular filter. A narrow spectral range of the light beam incident to the grating surface is reflected within a narrow acceptance angle when the Bragg conditions are met. RBGs are formed inside of glass bulk and, therefore, can contain a very large number of grating planes that allows fabrication of filters with unmatched ultra-narrow linewidth. On the contrary, the minimum linewidth of a thin film filter (TTF) is determined by the number of epitaxial layers that can be deposited on a substrate without degradation. Thus, the typical number of planes in a thin film filter is limited to about 100, while RBG can have more than 10,000 planes in one element. In Section 5 we will present a comparison of linewidths that can be obtained with glass holographic filters and TTFs.

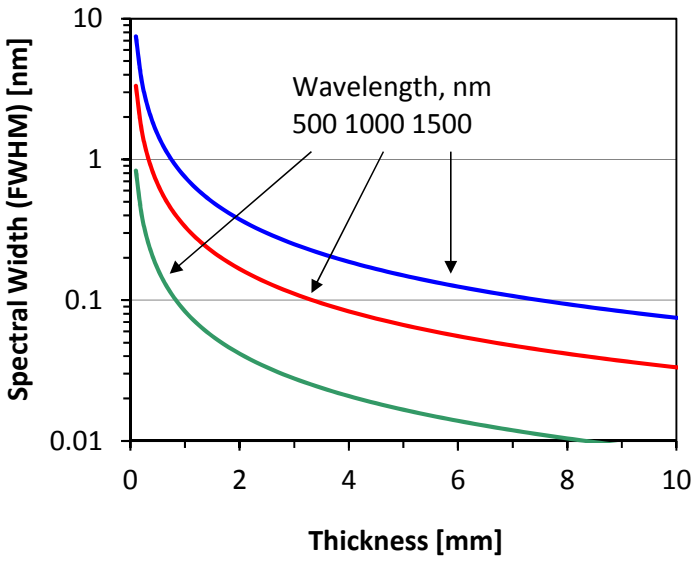

Figure 3. Dependence of RBG spectral width on the grating thickness at different wavelengths.

Another type of narrow band optical filters is holographic filters formed in dichroic gelatin or photopolymer materials. Even though the holographic recording technique used in polymer based VBGs is very similar to glass VBGs, practically achievable thickness of polymer materials is rather limited and, usually, can't be larger than 10's of μm. This limits the number of grating planes that can be formed in a polymer film and, accordingly, the minimum linewidths of the corresponding filters.

Dependence of spectral width of reflecting Bragg gratings on thickness is shown in Fig. 3. The spectral selectivity of a Bragg mirror drops if the wavelength decreases or the thickness of the grating increases. One can see that gratings with thicknesses of several millimeters have selectivity narrower than 0.01 nm in the UV spectral regions and 0.1 nm in the near IR region. RBGs with linewidth as narrow as 15-20 pm at 1 μm wavelength were experimentally demonstrated, which is equivalent to 5 GHz or 0.2 cm^{-1} bandwidth [2].

Another important characteristic of RBGs is their angular filtering capability or acceptance angle. The angular acceptance depends on the grating bandwidth, diffraction efficiency, thickness, and the incident angle. More details on reflecting VBG design and grating theory can be found elsewhere [18]. In the case of optical filters for spectral selection, angular acceptance defines the alignment accuracy that is needed to achieve proper grating performance. Fig. 4 presents angular acceptance in mrad at FWHM as a function of the grating deflection angle. It shows the dependences for four different diffraction efficiencies of RBGs at the same wavelength. The angular acceptance of a grating declines strongly as the deflection angle increases. Since it is favorable for optical filters in spectroscopic instruments to have larger acceptance angle, the gratings have to be designed with the smallest possible deflection angle. Also, it should be mentioned that filter linewidth and acceptance angle are related for a limited range of reflective index increment. Therefore, a filter with an ultra-narrow bandwidth has naturally a rather narrow acceptance angle as compared to wider band filters.

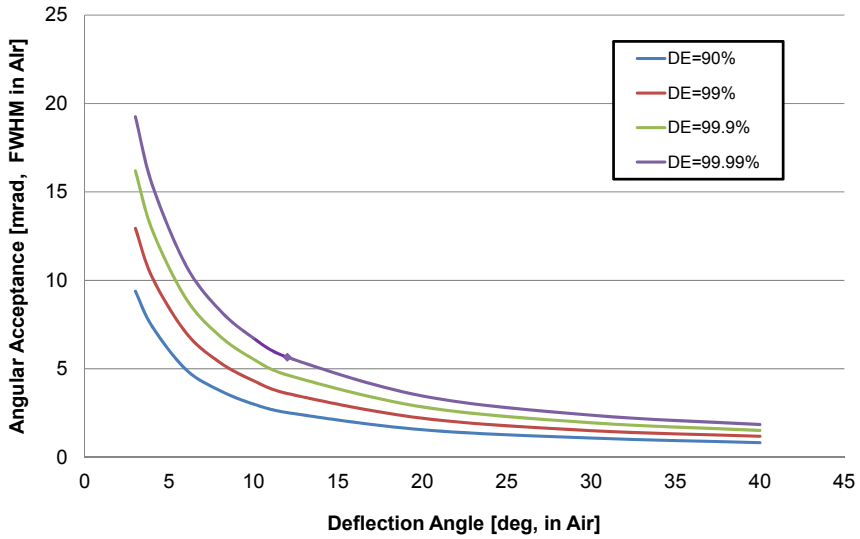

Figure 4. Angular acceptance of reflecting VBGs as a function of the light beam deflection angle for different grating diffraction efficiencies.

4. MULTIPLEXED VOLUME BRAGG GRATINGS

A unique feature of VBGs in PTR glass is a possibility to record a number of diffractive gratings in the same volume of glass, volume multiplexed VBGs (MUX-VBG). All these holograms are independent because no changes in refractive index and, therefore, no writing beam diffraction occur in the process of recording. All holograms appear only in the process of thermal development. Capacity for multiple hologram recording is determined by the maximum refractive index modulation. Thus, in the near IR region, a phase incursion sufficient for 100% diffraction efficiency can be achieved in a glass thickness of about 1 mm. This means that a PTR glass wafer of 5 mm can contain up to 5 RBGs with high diffraction efficiency. VBGs can be multiplexed in one volume for a variety of wavelength and angle combinations. Some examples of possible volume multiplexing configurations are shown in Fig. 5.

Fig. 5(a) shows the coplanar grating configuration for two different wavelengths. In this case two beams with different wavelengths have the same incident angle and are reflected at the same outgoing angle. This MUX-VBG configuration is used, for example, in notch and bandpass filters described below in Section 5. Configuration shown in Fig. 5(b) can be used for spectral beam combining, in which two beams at different wavelengths have different incident angles to the grating surface while they are reflected at the same output angle.

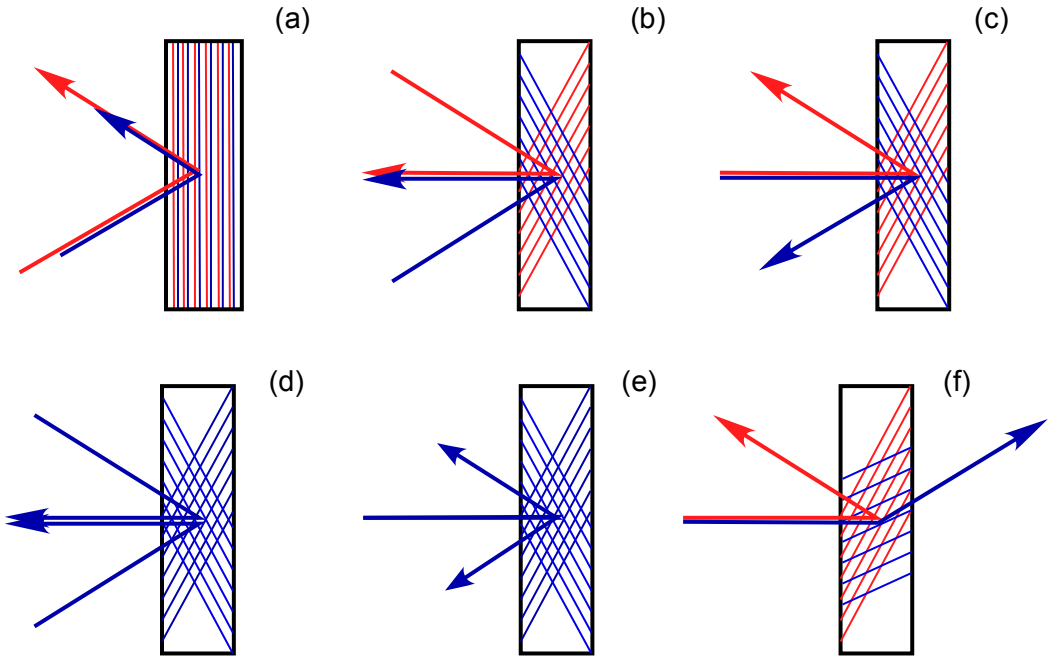

Figure 5. Selected variations of multiplexed VBGs: (a) multiband notch filter: beams at different wavelengths with the same incident and reflection angles; (b) spectral beam combiner: beams with different wavelengths and different incident angles reflected at the same output angle; (c) spectral beam splitter: beams with different wavelengths at the same incident angle reflected at different output angles; (d) beam combiner: beams with the same wavelength at different incident angles reflected at one output angle; (e) beam splitter: one beam splits into two beams at different output angles; (f) bi-directional beam splitter: multiplexed reflecting and transmitting gratings, only one combination is shown while multiple combinations are feasible.

The grating in Fig 5(c) can separate two beams at different wavelengths and reflect them in different directions. Similarly, reflecting and transmitting gratings can be multiplexed in the same volume and, thus, separate two beams by reflecting one beam and deflecting another as it is presented in Fig. 5(f). Obviously, any other beam that doesn't meet the Bragg conditions for the first two beams will pass through the gratings unaffected. The MUX-VBG configuration depicted in Fig. 5(d) can be used for coherent beam combining in which two coherent beams can be combined in one providing an elegant way of scaling high power laser systems. Fig. 5(e) represents a beam splitter, in which one beam can be split in two: in reflecting, transmitting or both geometries. Varying the diffraction efficiencies of the gratings in the splitter allows fabrication of splitter devices with different splitting ratios. Also multiband low efficiency RBGs can be used to stabilize diode lasers at multiple wavelengths [19].

5. ULTRA-NARROW BAND NOTCH FILTERS

In order to gain access to low frequency vibrations in Raman instruments, the Rayleigh light has to be rejected from the spectrometer as close as possible to the laser line. The ratio of useful signal to the Rayleigh light is typically around 60-70 dB and, therefore, the Rayleigh light has to be suppressed by at least six orders of magnitude to make the weak Raman modes detectable. The lowest measurable frequency of a Raman system is determined by the cut-off of the notch filters that are used to reject the direct light. Notch filters currently used in the industry have a cut-off frequency larger than 200 cm^{-1} and, thus, simultaneous measurements of Stokes anti-Stokes modes in such systems are limited to this frequency range. Edge filters can have a steeper slope than notch filters and enable Raman shift measurements down to

50-100 cm^{-1}. However, in this case, only measurements on one side of the laser line are possible restricting the feasibility monochromators, in which two stages (double subtractive spectrometer) are used solely to extract the direct Rayleigh light before entering the spectrometer. VBG based BragGrate™ notch filters (BNFs) make it possible to substitute double spectrometer stages with a filter set and, thus, make Raman systems with low frequency measurement capability lower cost and significantly smaller in size.

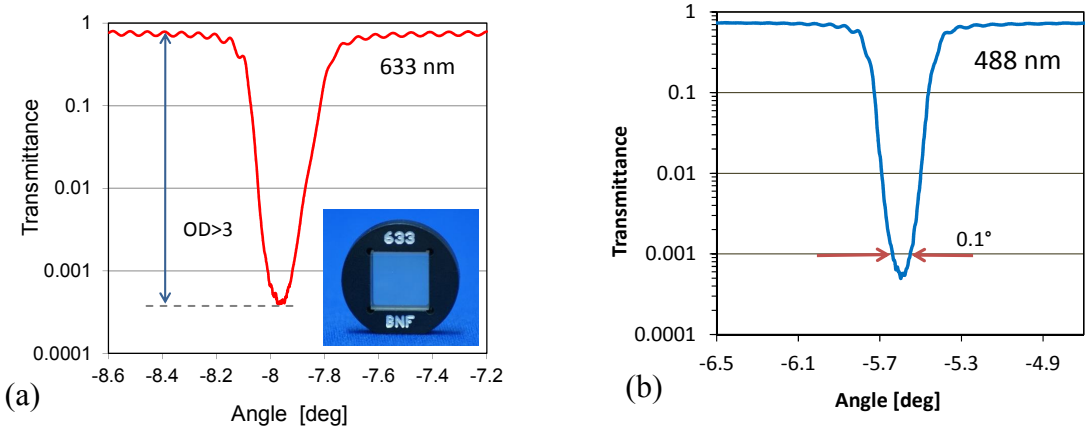

Figure 6. Angular scans of BNFs rated for optical density OD=3 at 633 nm (a) and 488 nm (b). The graphs show that the filters have to be aligned with the angle accuracy better than 0.1 degree to provide OD>3. The insert in (a) shows a photograph of 633 nm BNF with 12.5x12.5x3 mm^3 dimensions mounted in 25 mm round frame.

Reflecting volume Bragg gratings can be fabricated with diffraction efficiencies as high as 99.99% and the linewidth narrower than 1 cm^{-1} at FWHM that corresponds to 3-4 cm^{-1} cut-off frequency at -60 dB from maximum. This makes it a unique notch filter for Rayleigh light rejection with optical density OD=1-4 (10-40 dB supression) and the cut-off frequency as low as 3-4 cm^{-1} [20]. Single or multiplexed optical filters can be recorded in PTR glass with high optical density, narrow band, as well as low scattering and absorption losses by optimization of the PTR glass properties and the holographic recording procedure. The filters can be made for wavelengths covering almost full transparency window of PTR glass ranging from 400 nm to about 2 µm. The standard BNF wavelengths are tuned to the Raman laser source wavelengths such as 488, 514, 532, 633, 785, and 1064 nm. Figures 6 (a) and (b) show the transmission spectra of BNFs at 488 and 633 nm, respectively. The spectra were measured by angle scanning of the gratings. A spectral scan of a 785 nm BNF is presented in Fig. 7.

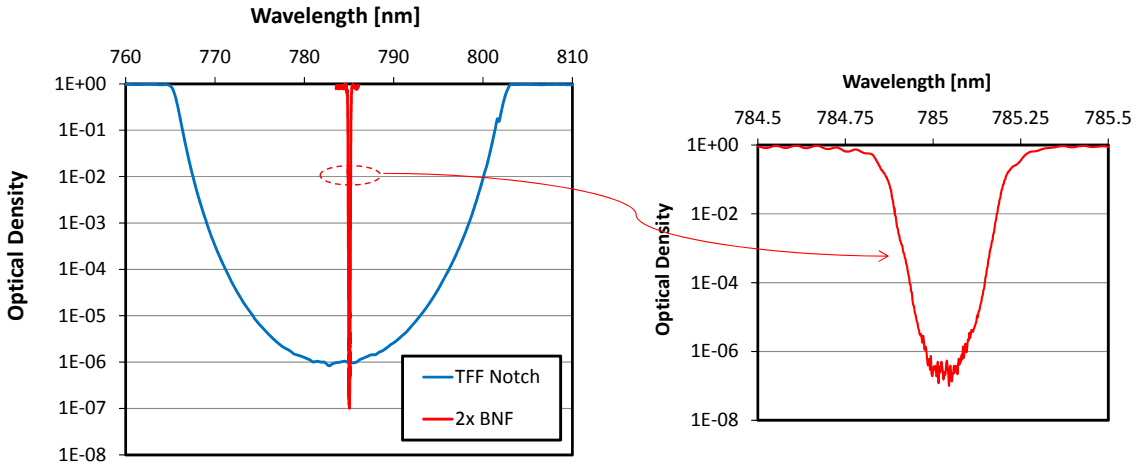

Figure 7. Spectral profiles of thin film notch filter (blue) and two aligned BragGrate™ Notch filters (BNFs). The BNF cut-off at 60 dB suppression is less than 5 cm^{-1}. The right panel shows the high resolution spectral profile of a 785 nm BNF.

Angular scans from Fig. 6 show an important parameter of a BNF, namely the angular alignment accuracy needed to obtain large suppression of the Rayleigh light. It can be seen in the figures that the transmittance decreases below 0.1% (OD>3) in the angular range of about 0.1 deg. This is the range in which the filter will provide Rayleigh light suppression higher than OD=3. The angle of minimum transmittance is coupled to a certain wavelength by the Bragg condition. Therefore, it should be emphasized that the filters are angle tunable in a rather large range of wavelengths. By changing the angle between the incident light beam and the filter, the reflected wavelength can be adjusted without loss of optical density in the range of about 3-5 nm.

Typical optical density of a single BNF in the wavelength range 400-1100 nm is 3-4. The maximum optical density that we demonstrated in a single grating was OD=5 at 785 nm. Most of Raman spectroscopy instruments require Rayleigh light suppression higher than 60 dB which can be obtained by sequential cascading of several BNFs. Figure 7 shows the spectral profile of two cascaded BNFs at 785 nm. The combined optical density of two filters is about 7. Also, for comparison we show a spectral profile of a high-end thin film notch filter (blue line in the left panel). One can see the dramatic reduction of the bandwidth that can be achieved with the VBG filter technology. This enables ultra-low frequency Raman measurements with single stage spectrometers.

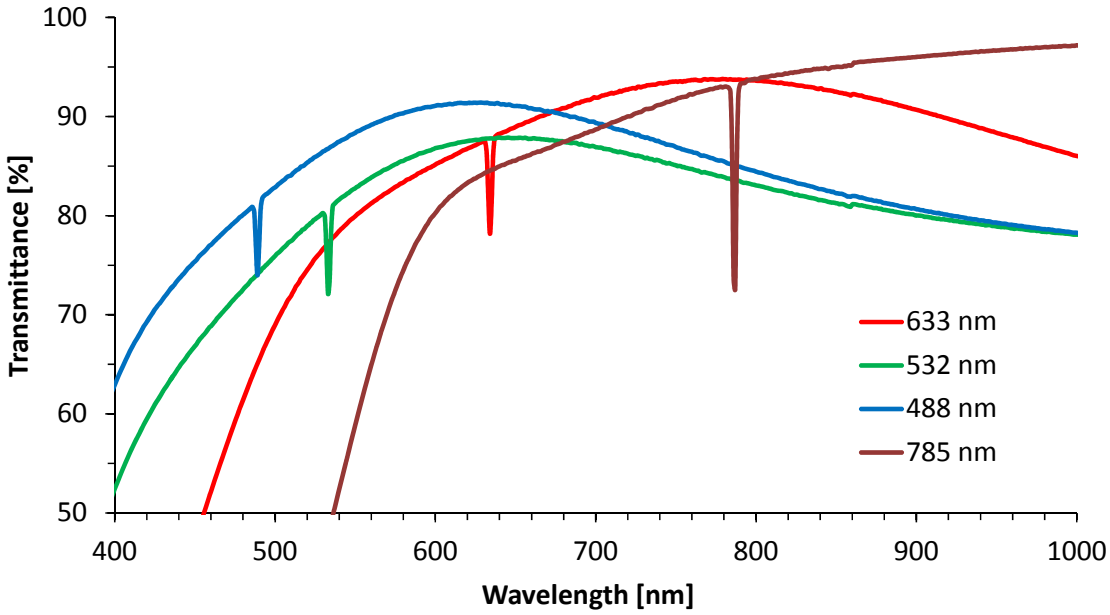

Figure 8. Transmission spectra of BNFs (with ARC) at different wavelengths.

Transmission spectra of various BNFs are presented in Fig. 8. Filters, rated for OD>3 at 488 nm, have characteristic losses of about 15-20%, 532 nm filters have similar losses of 15-20%, 633 nm filters have losses of 10-15%, while 785 nm have losses less than 10% for OD=3-4. BNF optical losses are primarily caused by the light scattering in the bulk of glass. The light scattering increases proportionally to the wavelength in the fourth power, λ^4. This results in decrease of the filter transmission at shorter wavelength. It should be noted that the measurements in Fig. 8 were performed with filters coated with anti-reflection (AR) films. The transmission variations of the AR coating contribute to the shape of the filter transmission curves. Actual transmission of BNFs at the marked resonant wavelengths is close to zero. The measured depth of sharp lines in transmission spectra (Fig. 8) is determined by spectral resolution and beam divergence in the spectrophotometer used for these measurements which are wider than spectral width and angular acceptance of BNFs.

Another type of a VBG filter for Raman spectroscopy applications is shown in Fig. 9. As we have discussed earlier in the paper, a set of BNFs can reject the Rayleigh light more than six orders of magnitude, as close as 5 cm^{-1} from the laser line. However, most of the laser sources used in Raman spectroscopy have noise stronger than -60 dB, such as amplified spontaneous emission (ASE), plasma lines, etc. Thus, in order to detect weak low-frequency Raman modes without

spectral noise, the laser line has to be cleaned to -60 dB and lower. Bandpass filters based on thin film technology could be used for this purpose; however, they do not remove noise closer than 100-200 cm^{-1} to the center wavelength of a laser. Similar to notch filters, the linewidth of a thin film bandpass filter is limited by the number of epitaxial layers that can be deposited without quality degradation and, thus, currently can only be as narrow as several nanometers.

A VBG in a reflecting geometry, BragGrate™ Bandpass Filter (BPF), can remove the spectral noise down to -60-70 dB, as it is shown in Fig. 9. A BPF is not an actual bandpass filter as it reflects the signal rather than transmits it; however, it does separate the useful signal from the noise and, thus, cleans up the laser line. A typical diffraction efficiency of a BPF is ~95% and, correspondingly, the loss of the useful signal is ~5%. The left panel of Fig. 9 demonstrates an example of how a BPF can be used in a Raman system. It should also be pointed out that standard BPF's deflection angles are around 20°. Filters with deflection angles up to 90° can be fabricated, but the angular acceptance of such filters will be narrowed (see Fig. 4), which is typically not preferred because of more stringent alignment requirements.

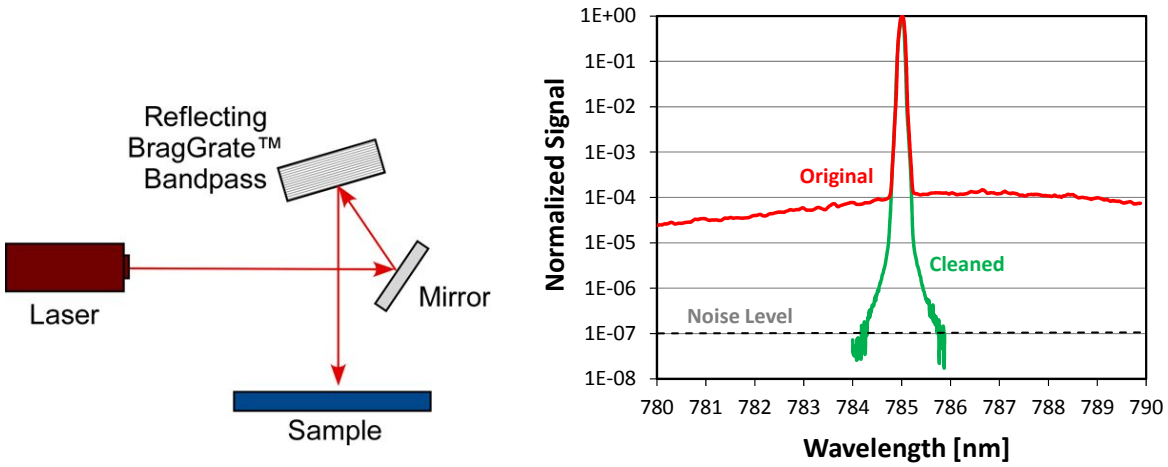

Figure 9. (left) Schematic presentation of possible assembly of reflecting BragGrate™ Bandpass filter; (right) Spectral profiles of 785 nm diode laser before and after the beam is cleaned with a VBG filter.

The most essential advantage of a VBG based clean-up filter is the narrow line width which matches the line widths of BNFs. Therefore, a BPF can clean the laser line and reduce the spectral noise below -70 dB with the same linewidth as the notch filters that are used in the same instrument to reject the laser line after its interaction with the studied sample. The right panel of Fig. 9 shows the original spectrum of a laser diode at 785 nm wavelength (red line) and the spectrum of a laser after cleaning it with a BragGrate™ Bandpass filter (green line).

As we discussed in Section 4, volume multiplexing of high efficiency RBGs enables fabrication of several BNFs or BPFs at different wavelengths in a single glass plate. The VBG glass and recording technologies have to be highly optimized to achieve such capability. First multiband high efficiency filters with such parameters are presented in this work. Fig. 10 shows a transmission spectrum of a multiband BNF for 532 and 633 nm wavelengths.

In Fig. 10, the blue transmission curve was measured with a spectrophotometer and indicates the spectral position of the two gratings formed in the multiband filter. Higher resolution scanning with optical spectrum analyzer was used to map the filter transmission around the grating wavelengths. The inserts in Fig. 10 demonstrate that both filters at 532 and 633 nm have optical density of 3 which corresponds to diffraction efficiency of 99.9%. BPFs, which typically have diffraction efficiencies of only 95%, can be fabricated by this technique as well. In fact, if BNF multiplexing is currently limited to two wavelengths per filter, four to five BPFs can be formed in one filter due to the lower diffraction efficiency requirement. The practical limits of VBG volume multiplexing were described in Section 4. Multiband BNFs can have any combination of wavelengths in the range from 400-2000 nm; however, the most useful combination may be 488 and 514 nm as it covers main wavelengths of Ar-ion lasers frequently used as Raman laser sources.

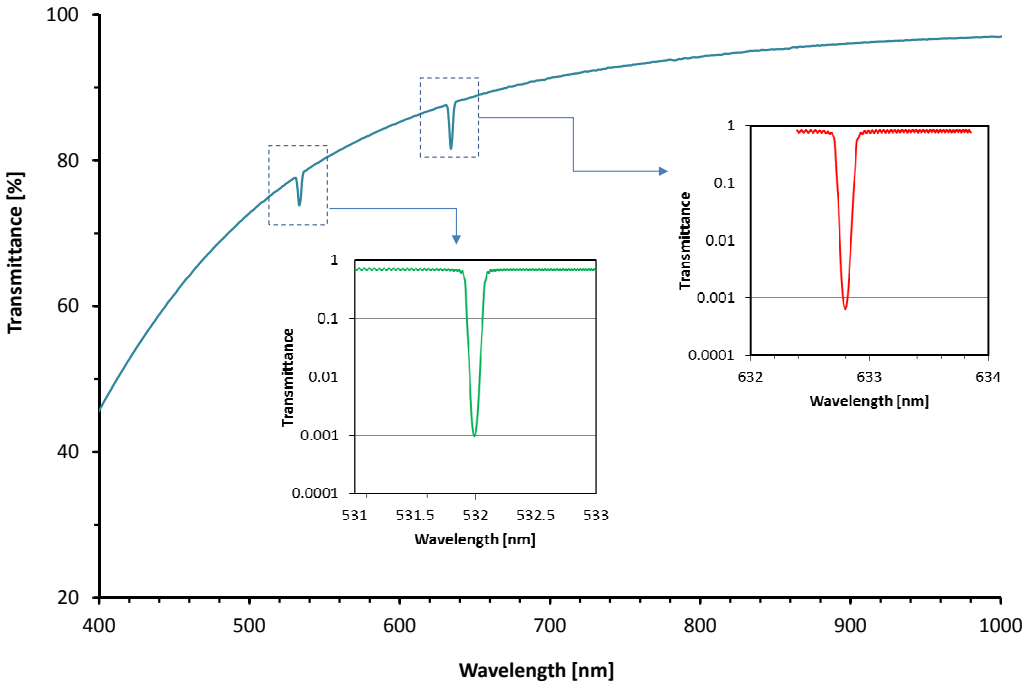

Figure 10. Transmission spectrum of a multiplexed BragGrate™ notch filter for 532 and 633 nm. Two high efficiency gratings with diffraction efficiency larger than 99.9% are recorded in the same glass substrate with identical incident and output angles. The inserts of the figure depict spectral profiles of the two gratings.

6. ULTRA-LOW FREQUENCY RAMAN MEASUREMENTS WITH VBG FILTERS

The ultra-narrow notch filter performance was tested in a single stage monochromator Raman systems to gain access to Raman frequencies very close to the laser line at 488, 532, 633, and 785 nm wavelengths. LabRamHR Raman system from Horiba Scientific was employed for the experiments and sets of three OD3 BragGrate™ notch filters at each wavelength were used to reject the corresponding laser lines. The schematics of the three filter set positioning in the system is shown in Fig. 11. The first BNF filter is deployed in a dual function: 1) to inject the light beam in the microscope chamber, thus, also cleaning up the laser beam from spectral noise (see Fig. 9); and 2) as a notch filter rejecting the Rayleigh light reflected from the sample. The other two BNFs are used as regular notch filters to stop the Rayleigh light from entering the spectrometer.

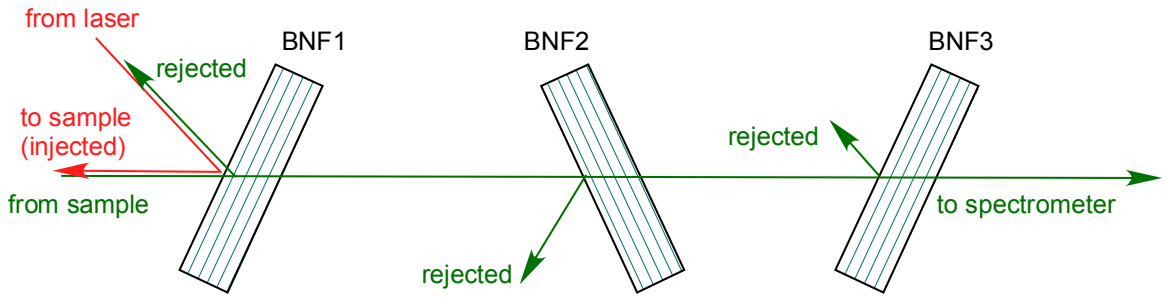

Figure 11. Schematics of filter positioning in a Raman system for ultra-low frequency measurements. BNF1 is used in the inject/reject configuration, while BNF2 and BNF3 reject the Rayleigh light from the spectrometer. Depending on the system, BNF3 may be not needed.

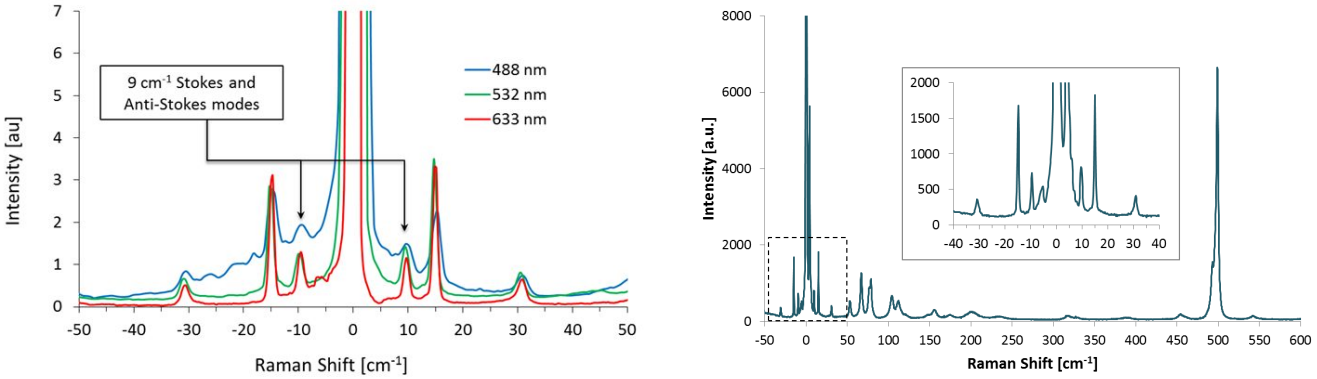

Figure 12. Ultra-low frequency Raman spectra: (left) Raman spectra of L-Cystine measured at LabRamHR with a single stage monochromator and a set of BNFs at 488, 532, and 633 nm; (right) L-Cystine ULF Raman measurements with a 785 nm laser source and corresponding BNFs.

The measured ultra-low frequency (ULF) Raman spectra are presented in Fig. 12. The left panel of Fig. 12 shows ULF Raman measurements on L-Cystine as a probe material. The measured spectra clearly show both Stokes and Anti-Stokes L-Cystine bands at 9 cm^{-1} which were simultaneously measured with a single stage spectrometer at all three wavelengths. The right panel of Fig. 12 presents the ULF Raman measurement of L-Cystine sample using a diode laser source at 785 nm and the corresponding BNFs. Similar measurements were also successfully demonstrated with a 1064 nm laser source. The cut-off frequency of BragGrate™ notch filters is 3-4 cm^{-1}, therefore, measurements of vibrational modes down to 5 cm^{-1} are feasible and have been demonstrated.

Fig. 13 depicts low-wavenumber Raman measurements conducted with a single monochromator stage LabRamHR instrument and a set of dual-band BPFs and BNFs at 532 and 633 nm. The left and right panels of the figure show the comparison of the dual-band filter measurements with those performed with single-band filter sets. The spectra presented clearly show that there is no difference between the single- and dual-band filters in terms of resolution or low frequency access; however, multiband filters show slightly reduced Raman mode intensities.

Thus, multiband VBG filters provide an exclusive possibility to conduct ultra-low frequency Raman measurements at different wavelengths using the same set of bandpass and notch filters.

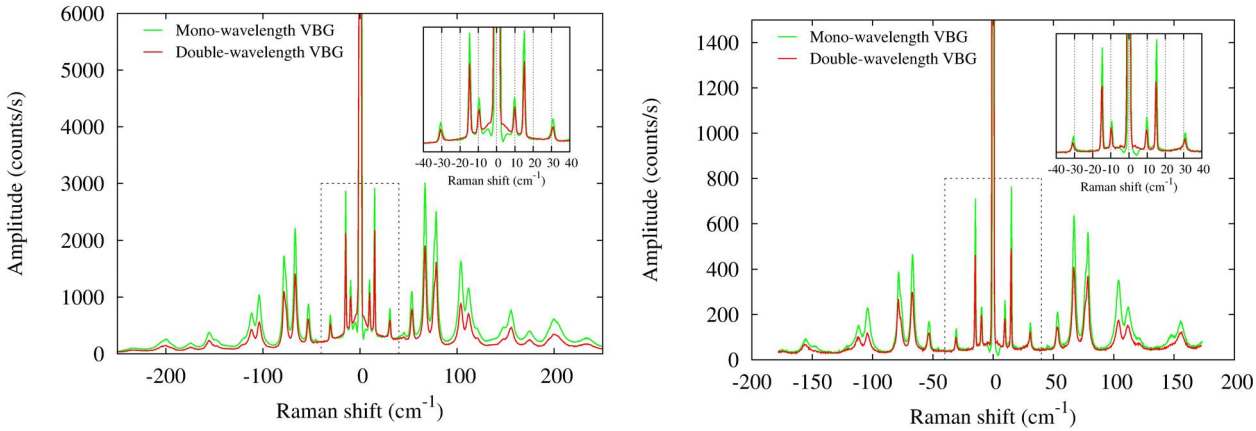

Figure 13. Ultra-low frequency Raman spectra of L-Cystine measured with a single stage spectrometer and one set of multiband BragGrate™ Notch Filters at 532 (left) and 633 nm (right).

7. SUMMARY

In this paper we reviewed recent advances in volume Bragg grating technologies that enabled fabrication of very high efficiency reflecting gratings with ultra-narrow linewidth. Such gratings can be used as unique optical filters in Raman spectroscopy instruments dramatically improving the capability of those instruments to access low-frequency Raman bands down to 5 cm^{-1}. In contrast to frequently used edge filters, VBG based notch filters enable simultaneous measurements of low wavenumber Stokes and anti-Stokes modes while multiband BragGrate™ filters allow using of one filter set for different wavelength laser sources.

REFERENCES

[1] Glebov, L. B., "High brightness laser design based on volume Bragg gratings," Proc. SPIE 6216, 621601 (2006).
[2] Gourevitch, A., Venus, G., Smirnov, V. and Glebov, L., "Efficient pumping of Rb vapor by high-power volume Bragg diode laser," Opt. Lett. 32, 2611-2613 (2007).
[3] Jelger, P., Pasiskevicius, V. and Laurell, F. "Narrow linewidth high output-coupling dual VBG-locked Yb-doped fiber laser," Opt. Express 18, 4980-4985 (2010).
[4] Wang, F., Shen, D., Fan, D. and Lu, Q. "Spectrum narrowing of high power Tm: fiber laser using a volume Bragg grating," Opt. Express 18, 8937-8941 (2010).
[5] Chung, T., Rapaport, A., Smirnov, V., Glebov, L., Richardson, M. and Bass, M., "Solid-state laser spectral narrowing using a volumetric photothermal refractive Bragg grating cavity mirror," Opt. Lett. 31, 229-231 (2006).
[6] Vorobiev, N., Glebov, L. and Smirnov, V., "Single-frequency-mode Q-switched Nd:YAG and Er:glass lasers controlled by volume Bragg gratings," Opt. Express 16, 9199-9204 (2008).
[7] Liao, K.-H., Cheng, M.-Y., Flecher, E., Smirnov, V. I., Glebov, L. B. and Galvanauskas, A., "Large-aperture chirped volume Bragg grating based fiber CPA system," Opt. Express 15, 4876-4882 (2007).
[8] Moulton, P. and Slobodchikov, E., "1-GW-Peak-Power, Cr:ZnSe Laser," in CLEO:2011 - Laser Applications to Photonic Applications, OSA Technical Digest (Optical Society of America, 2011), paper PDPA10.
[9] Sevian, A., Andrusyak, O., Ciapurin, I., Venus, G., Smirnov, V. and Glebov L., "Efficient Power Scaling of Laser Radiation by Spectral Beam Combining," Opt. Lett. 33, 384-386 (2008).
[10] Andrusyak, O., Smirnov, V., Venus, G., Rotar, V., and Glebov, L., "Spectral Combining and Coherent Coupling of Lasers by Volume Bragg Gratings," IEEE Journal of Selected Topics in Quantum Electronics, 15, 344-353 (2009).
[11] Glebov, A. L., Smirnov, V. I., Lee, M. G., Glebov, L. B., Sugama, A., Aoki, S., and Rotar, V., "Angle Selective Enhancement of Beam Deflection in High-Speed Electrooptic Switches," Photonics Technology Letters, IEEE; 19, 701-703 (2007).
[12] Glebov, L., "Fluorinated silicate glass for conventional and holographic optical elements", Proc. SPIE 6545, 654507 (2007).
[13] Ciapurin, I. V., Glebov, L. B. and Smirnov, V. I. "Modeling of Gaussian beam diffraction on volume Bragg gratings in PTR glass", Proc. SPIE 5742, 183 (2005).
[14] Glebov, A., Mokhun, O., Smirnov, V., Glebov L., Rapaport, A., Roussel, B., Reich, H.-J. and Adar, F., Novel volume Bragg grating notch filters for ultralow-frequency Raman measurements," The 3rd Scientific EOS Annual Meeting (EOSAM 2010), paper 4007.
[15] Rapaport, A., Roussel, B., Reich, H.-J., Adar, F., Glebov, A., Mokhun, O., Smirnov, V. and Glebov L., "Very Low Frequency Stokes and Anti-Stokes Raman Spectra Accessible with a Single Multichannel Spectrograph and Volume Bragg Grating Optical Filters," Abstracts of ICORS (2010), paper TP13-113 (Raman Instrumentation).
[16] Tan, P.-H. et al., "The shear mode of multilayer graphene," Nature Materials 11, 294–300 (2012).
[17] Ibanez, J., et al., "Raman scattering by folded acoustic phonons in InGaN/GaN superlattices," J. Raman Spectrosc. 43, 237-240 (2012).
[18] Ciapurin, I. V., Drachenberg D. R., Smirnov, V. I., Venus, G. B. and Glebov L. B., "Modeling of phase volume diffractive gratings, part 2: reflecting sinusoidal uniform gratings (Bragg mirrors)," Opt. Eng. 51, in print (2012).
[19] Zolotovskaya, S.A., Smirnov, V.I. ; Venus, G.B. ; Glebov, L.B. ; Rafailov, E.U., "Two-Color Output From InGaAs Laser With Multiplexed Reflective Bragg Mirror," IEEE Phot. Tech. Lett. 21, 1093-1095 (2009)
[20] http://www.optigrate.com/BragGrate_Notch.html